Molecular Medicine

Induction of Steatohepatitis (NASH) with Insulin Resistance in Wild-type B6 Mice by a Western-type Diet Containing Soybean Oil and Cholesterol

Janin Henkel,[1] Charles Dominic Coleman,[1] Anne Schraplau,[1] Korinna Jöhrens,[2] Daniela Weber,[7,10] José Pedro Castro,[6,7,8,9] Martin Hugo,[7] Tim Julius Schulz,[3,6] Stephanie Krämer,[4] Annette Schürmann,[5,6] and Gerhard Paul Püschel[1]

[1]Department of Nutritional Biochemistry, Institute of Nutritional Science, University of Potsdam, Nuthetal, Germany; [2]Institute of Pathology, Charité University Hospital Berlin, Berlin, Germany; [3]Department of Adipocyte Development and Nutrition, German Institute of Human Nutrition, Nuthetal, Germany; [4]Animal Facility, German Institute of Human Nutrition, Nuthetal, Germany; [5]Department of Experimental Diabetology, German Institute of Human Nutrition, Nuthetal, Germany; [6]German Center for Diabetes Research, München-Neuherberg, Germany; [7]Department of Molecular Toxicology, German Institute of Human Nutrition, Nuthetal, Germany; [8]Faculty of Medicine, Department of Biomedicine, University of Porto, Porto, Portugal; [9]Aging and Stress Group, Institute for Innovation and Health Research, Porto, Portugal; and [10]NutriAct – Competence Cluster Nutrition Research Berlin-Potsdam, Nuthetal, Germany

Nonalcoholic fatty liver disease (NAFLD) and nonalcoholic steatohepatitis (NASH) are hepatic manifestations of the metabolic syndrome. Many currently used animal models of NAFLD/NASH lack clinical features of either NASH or metabolic syndrome such as hepatic inflammation and fibrosis (e.g., high-fat diets) or overweight and insulin resistance (e.g., methionine-choline-deficient diets), or they are based on monogenetic defects (e.g., ob/ob mice). In the current study, a Western-type diet containing soybean oil with high n-6-PUFA and 0.75% cholesterol (SOD + Cho) induced steatosis, inflammation and fibrosis accompanied by hepatic lipid peroxidation and oxidative stress in livers of C57BL/6-mice, which in addition showed increased weight gain and insulin resistance, thus displaying a phenotype closely resembling all clinical features of NASH in patients with metabolic syndrome. In striking contrast, a soybean oil–containing Western-type diet without cholesterol (SOD) induced only mild steatosis but not hepatic inflammation, fibrosis, weight gain or insulin resistance. Another high-fat diet, mainly consisting of lard and supplemented with fructose in drinking water (LAD + Fru), resulted in more prominent weight gain, insulin resistance and hepatic steatosis than SOD + Cho, but livers were devoid of inflammation and fibrosis. Although both LAD + Fru– and SOD + Cho–fed animals had high plasma cholesterol, liver cholesterol was elevated only in SOD + Cho animals. Cholesterol induced expression of chemotactic and inflammatory cytokines in cultured Kupffer cells and rendered hepatocytes more susceptible to apoptosis. In summary, dietary cholesterol in the SOD + Cho diet may trigger hepatic inflammation and fibrosis. SOD + Cho–fed animals may be a useful disease model displaying many clinical features of patients with the metabolic syndrome and NASH.

Online address: http://www.molmed.org
doi: 10.2119/molmed.2016.00203

INTRODUCTION

Apart from being the central organ for maintenance of glucose homeostasis (1), the liver plays a pivotal role in lipid metabolism (2). All lipoproteins, with the exception of chylomicrons, are generated or metabolized by the hepatocytes, which, for the purpose of regulating whole-body lipid homeostasis, can serve as an intermediary triglyceride storage compartment. Whereas transient triglyceride storage in the hepatocyte is a physiological process, disproportionate and protracted triglyceride accumulation in hepatocytes is a pathological phenomenon, called steatosis. Hepatic steatosis is the consequence of a prolonged excessive supply of calories in general or lipids in particular. Hepatic steatosis is one feature of nonalcoholic fatty liver disease (NAFLD), which can be complicated by low-grade inflammation and fibrosis in nonalcoholic steatohepatitis (NASH), which in the long run can give

Address correspondence to *Janin Henkel, Department of Nutritional Biochemistry, Institute of Nutritional Science, University of Potsdam, Arthur-Scheunert-Allee 114-116, D-14558, Nuthetal, Germany. Phone: (+49)-33200-885285; Fax: (+49)-33200-885541; E-mail: jhenkel@uni-potsdam.de.*
Submitted September 28, 2016; Accepted for Publication March 15, 2017; Published online (www.molmed.org) March 21, 2017.

Feinstein Institute for Medical Research
Northwell Health™

rise to liver cirrhosis and hepatocellular carcinoma (3). As a consequence of the worldwide epidemic of overweight and obesity resulting from easy access to energy-dense, highly palatable food and a predominantly sedentary lifestyle, the prevalence of NAFLD/NASH is continually increasing, and it is now the most common cause of chronic liver disease (4). NAFLD is viewed as a hepatic manifestation of the metabolic syndrome (5). It is associated with impaired glucose tolerance and dyslipidemia. While steatosis is always present in NAFLD, only a minor fraction of all patients develop the more severe forms, and it is currently not clear whether progression from steatosis to NASH with inflammation and fibrosis is a temporal continuum or the result of multiple parallel injuring impacts, of which triglyceride overload is but one (6). Since taking liver biopsies repeatedly from the same patient to study the mechanisms underlying disease progression is not feasible, animal models that resemble the course of human NASH development are needed. However, many animal models currently used to study NAFLD fail to reproduce all clinical, biochemical and morphological features of human NASH (7). Genetic obesity models, such as *ob/ob* or *db/db* mice, display steatosis and are insulin resistant but appear to be protected from the development of inflammation and fibrosis (8). Similarly, rats or mice fed a high-fat diet gain weight, are insulin resistant and rapidly develop hepatic steatosis, but develop little or no hepatic inflammation and fibrosis (9). On the other hand, administration of a choline-methionine-deficient diet, a frequently used feeding model, results in hepatic steatosis with inflammation and fibrosis. However, in contrast to patients suffering from the metabolic syndrome, animals fed a choline-methionine-deficient diet lose weight and are not insulin resistant (10). When added to a high-fat diet, both fructose (11) and cholesterol (12) as well as increased n-6-polyunsaturated fatty acid (n-6-PUFA) in the fat content (13,14) seem to favor development of liver steatosis and insulin resistance or inflammation and fibrosis. Therefore, in the current study, three high-fat diets differing in their fatty acid composition as well as cholesterol and fructose content were compared for their impact on weight gain, insulin resistance and development of NASH.

MATERIALS AND METHODS

All chemicals were of analytical or higher grade and obtained from local providers unless otherwise stated.

Animals and Experimental Design

Male C57BL/6J mice (littermates; Janvier Labs, Le Genest Saint Isle, France) were housed in type II cages (5 per cage) at 20 ± 2°C with a 12 h light-dark cycle. Mice were randomly assigned to one of the following diet groups (5 mice per group) with free access to food and liquid for 20 wks: (1) standard chow diet with 3.3 g/100 g fat (STD, V153 R/M-H; Ssniff, Soest, Germany), (2) Western-type diet containing 25 g/100 g n-6-PUFA-rich soybean oil, (3) Western-type diet containing 25 g/100 g n-6-PUFA-rich soybean oil + 0.75% cholesterol (SOD and SOD + Cho, respectively; Altromin, Lage, Germany), (4) high-fat diet containing 21 g/100 g lard and 3 g/100 g soybean oil (LAD, D12451; Research Diets, New Brunswick, NJ, USA) and 5% fructose in the drinking water (LAD + Fru). Detailed diet composition is shown in Table 1. Mice had access to wooden gnawing sticks to avoid excessive tooth growth. Body weight was measured weekly. Mice were killed by cervical dislocation after isoflurane anesthesia. Serum and organs were snap-frozen in liquid nitrogen and stored at –70°C for biochemical analysis, and aliquots of the organs were fixed for histological examination. The principles of laboratory animal care were followed. Treatment of the animals followed the German animal protection laws and the study was performed with permission of the state animal welfare committee (LUGV Brandenburg, V3-2347).

Body Composition and *In Vivo* Experiments

Body fat content was measured *in vivo* at the beginning and the end of the diet intervention by nuclear magnetic resonance spectroscopy (EchoMRI 2012 Body Composition Analyzer, Houston, TX, USA). Oral glucose tolerance test was performed during wk 18, after an overnight fast, by oral gavage of glucose (2 mg/kg body weight). Insulin tolerance test was performed during wk 19, after 3 h fasting, with intraperitoneal injection of insulin (0.25 U/kg body weight, Novo Nordisk, Mainz, Germany). Glucose and insulin levels were measured at the times indicated by a glucose sensor (Breeze2, Bayer, Berlin, Germany) or an insulin enzyme-linked immunosorbent assay kit (#90010, Crystall Chem, Downers Grove, IL, USA).

Serum and Tissue Analysis

Serum parameters were quantified by an automated analyzer (Cobas Mira S, Hoffmann-La Roche, Basel, Switzerland) with the appropriate commercially available reagent kits. Liver triglycerides and cholesterol were determined by triglyceride assay (Randox, Crumlin, UK) and cholesterol liquicolor (HUMAN, Wiesbaden, Germany). Malondialdehyde was quantified by high-performance liquid chromatography with fluorescence detection in frozen liver tissue homogenized in 50 mM cold phosphate buffer. Briefly, homogenates were derivatized with thiobarbituric acid and further proceeded as described elsewhere (15).

Hepatic Histology

Formalin-fixed and paraffin-embedded liver sections (2–5 μm) were stained with hematoxylin and eosin, Masson's trichrome or Sirius Red (all from Sigma-Aldrich, Taufkirchen, Germany). Immunohistochemistry analysis was performed with anti-F4/80 antibody (AbD Serotec, Bio-Rad, Munich, Germany). Terminal deoxynucleotide transferase dUTP Nick-End Labeling (TUNEL) assay was performed with the Apo-BrdU-IHC™

Table 1. Composition of mouse diets used in the feeding experiment.

	STD	SOD	SOD + Cho	LAD + Fru
Metabolizing energy (kcal/g)	3.06	4.50	4.50	4.73
Energy from carbohydrates (%)	65	40	40	35
Energy from protein (%)	23	17	17	20
Energy from fat (%)	8	43	43	45
Cholesterol (%)	0.00	0.00	0.75	0.02
Fructose in drinking water (%)	0	0	0	5
Fatty acid composition				
Saturated fatty acids (g/100g)	0.55	4.00	4.00	7.26
Monounsaturated fatty acids (g/100g)	0.64	5.75	5.75	8.69
Polyunsaturated fatty acids (g/100g)	2.01	14.50	14.50	6.36

STD, standard diet; SOD, soybean oil diet; SOD + Cho, soybean oil diet + cholesterol; LAD + Fru, lard diet + fructose

kit (Bio-Rad). Histological steatosis, inflammation and fibrosis were graded according to the NASH activity score (16,17) by a liver pathologist (KJ) blinded to the diet. Sirius Red staining was quantified by ImageJ software (18) in images of 11 randomly chosen fields of each liver containing no blood vessels (central veins or portal fields).

Real-time Reverse Transcription Polymerase Chain Reaction Analysis

RNA isolation, reverse transcription and quantitative polymerase chain reaction were performed as previously described (19). Oligonucleotide sequences are listed in Supplementary Table S1. Results are expressed as relative gene expression normalized to expression levels of reference genes (*Hprt*, *Eef2* and *Srsf4* [liver] or *β-actin* [*Actb*; Kupffer cells, hepatocytes]) according to the formula: fold induction = $2^{\text{(control-treated) gene of interest}} / 2^{\text{(control-treated) reference gene(s)}}$.

Western Blot Analysis and Oxyblot

Western blot was performed as previously described (20) with anti-Prx-SO_3 (Abcam, Cambridge, UK), anti-IRS-1 and anti-IRS-2 antibodies (NEB, Frankfurt am Main, Germany) as well as FastGreen staining (Sigma-Aldrich) as a loading control. Oxyblot analysis was done as previously described (21) with anti-DNP antibody (Sigma-Aldrich). Visualization of immune complexes was performed by using chemoluminescence reagent in the ChemiDoc™ Imaging System with ImageLab software (Bio-Rad).

Hepatic Glycogen Quantification

Frozen liver tissue was homogenized in 3.6 % $HClO_4$ by sonication. Homogenate or glycogen standards were incubated with 2 M $KHCO_3$, 1 M $C_2H_3NaO_2$ with or without 2 mg/mL amyloglucosidase (Sigma-Aldrich) for 2 h at 37°C. Glucose content was determined in supernatants using Fluitest® GLU kit (drepharm, Rüdersdorf, Germany).

Isolation and Cultivation of Murine Hepatocytes and Kupffer Cells

Hepatocytes and Kupffer cells were isolated from STD-fed male C57BL/6J mice as previously described (22,23), with minor modifications, using 16.6 μg/mL Liberase™ (Roche, Berlin, Germany). Density gradient–purified Kupffer cells were cultured for 44 h in low-endotoxin RPMI medium (Biochrom AG, Berlin, Germany) containing 1% antibiotics and 30% fetal calf serum and subsequently incubated for 8 h with 1 mg/mL cholesterol crystals (24). Percoll-purified hepatocytes (20) were cultured for 44 h in Williams E medium (Sigma-Aldrich) containing 1% antibiotics, 100 nM dexamethasone and 0.5 nM insulin (Sigma-Aldrich) as well as 4% fetal calf serum for the first 2 h.

Hepatocyte Apoptosis Assay

Cultured hepatocytes were exposed to 25 μg/mL cholesterol crystals (dissolved in dimethyl sulfoxide), 1 ng/mL TNFα (Peprotech, Hamburg, Germany) and 300 nM actinomycin D (Axxora, Loerrach, Germany) in Williams E medium containing 1% antibiotics and 0.5 nM insulin for 8 h and harvested using lysis buffer (25 mM HEPES pH 7.5, 5 mM $MgCl_2$, 1 mM EGTA, 0.1 % Triton X-100 and protease inhibitors). The cell supernatants were diluted 1/10 in assay buffer (50 mM HEPES pH 7.5, 1% sucrose, 0.1% CHAPS, 10 mM DTT and 50 μM DEVD-AMC). Fluorescence was measured every 1 min for 30 min (excitation/emission 390/460 nm) and normalized to protein content (25).

Statistical Analysis

Statistical analysis was performed as detailed in the figure legends.

All supplementary materials are available online at www.molmed.org.

RESULTS

Induction of NASH by Dietary Cholesterol in Soybean Oil Diet

Animals were fed (1) a standard chow diet (8% of the calories derived from fat) as a control (STD), (2) a Western-type diet with 43% of the calories derived from soybean oil (25 g/100 g) with a high content of n-6-PUFAs such as linoleic acid (13,2 g/100 g) (soybean oil diet, SOD), (3) a Western-type diet similar to (2) that additionally contained 0.75% cholesterol (soybean oil + cholesterol diet, SOD + Cho) and (4) a lard-containing high-fat diet with 45% of the calories mainly from fat with saturated fatty acids (21 g/100 g lard) and a minor fraction of n-6-PUFA (3 g/100 g soybean oil) supplemented with 5% fructose in drinking water (lard + fructose diet, LAD + Fru) (for details, see Table 1). Animals that received either of the diets with higher fat content suffered from

triglyceride accumulation in the liver (Figures 1A and C). Steatosis was mildest in SOD-fed animals and more pronounced in SOD + Cho– and LAD + Fru–fed animals (Figure 1C). Neither SOD-fed nor LAD + Fru–fed animals showed signs of tissue damage or inflammation. By contrast, SOD + Cho–fed animals showed ballooning (hypertrophy), immune cell infiltration and fibrosis (Figure 1A). A prominent histological phenomenon is accumulation of hypertrophic hepatocytes surrounded by F4/80-positive macrophages and collagen accumulation in structures similar to crown-like structures in inflamed adipose tissue (Figure 1A, third line). The histological findings were summarized in the NASH activity score according to Kleiner and Brunt (16) with adaptations to the rodent model proposed by Liang *et al.* (17) This score takes into consideration steatosis on a scale of 0 to 3, ballooning (hypertrophy) on a scale of 0 to 3, inflammation on a scale of 0 to 3 and fibrosis on a scale of 0 to 4 (Figure 1B). All animals receiving STD, SOD or LAD + Fru showed signs of mild fibrosis (stage 1A), most likely attributable to the advanced age of the mice. While due to the mild fibrosis, the median NASH score of STD- and SOD-fed animals was 1; SOD + Cho–fed animals had a median NASH score of 8, with higher values for steatosis, inflammation and fibrosis than any of the other groups, thus classifying the liver pathology in this group clearly as active NASH. By contrast, the NASH score of LAD + Fru–fed animals was only 3 and reflected almost entirely the steatosis; no signs of inflammation or fibrosis exceeding the control group were observed in this group (Figure 1B).

Liver triglyceride and cholesterol content were also determined biochemically. While triglyceride content was not statistically significantly elevated in SOD-fed animals compared with STD, it was increased more than 10-fold in animals receiving SOD + Cho or LAD + Fru (Figure 1C). Tissue cholesterol in liver was elevated only in SOD + Cho–fed animals (Figure 1D) and in none of the other groups. Although animals that received LAD + Fru had the highest plasma cholesterol levels (Supplementary Table S2, upper panel), their hepatic cholesterol levels were not elevated.

Impact of Dietary Cholesterol in Soybean Oil Diet on Lipid Peroxidation and Oxidative Stress

Malondialdehyde, which is produced during peroxidation of PUFA, was significantly increased in liver homogenates of SOD-fed mice, irrespective of the additional presence of cholesterol (Figure 2A). Malondialdehyde was not detected in liver homogenates of mice fed LAD + Fru, indicating that enhanced lipid peroxidation prevailed in both the SOD- and SOD + Cho–fed groups. While an increase in malondialdehyde can be found in response to relatively mild oxidative stress, oxidized peroxiredoxins (Prx) (26) and protein carbonyls (proteins with oxidized residues such as aldehydes and ketones) (15) are markers for severe oxidative stress. Elevated levels of hyperoxidized peroxiredoxin (Prx-SO_3) and protein carbonyl were only detectable in liver homogenates of SOD + Cho–fed mice, not in livers of mice fed SOD without cholesterol or LAD + Fru (Figure 2B and C). Thus high PUFA in the soybean oil diet increased lipid peroxidation, while the combination of high PUFA and cholesterol in SOD + Cho amplified the oxidative stress level, causing irreversible protein modifications. The ensuing grave tissue damage resulted in an increase in hepatocyte apoptosis as detected by TUNEL staining. Augmented numbers of TUNEL-positive hepatocytes were solely found in livers of SOD + Cho–fed mice (Figure 2D). In further support, *Fas ligand*, a marker of apoptosis, was also enhanced in livers of this diet group (Figure 3B).

Induction of Biochemical Signs of Liver Damage and Inflammation by Dietary Cholesterol in Soybean Oil Diet

The histological signs of liver damage were also reflected in plasma levels of alanine-aminotransferase, which was normal in STD-, SOD- and LAD + Fru–fed animals (23.48 ± 2.74, 19.23 ± 5.29 and 23.85 ± 4.95, respectively) but was elevated in SOD + Cho–fed animals (44.46 ± 8.34, $p = 0.072$ versus control, $p < 0.05$ versus SOD, one-way analysis of variance) (Supplementary Table S2, lower panel). Similarly, biochemical signs of liver cell fibrosis, apoptosis and ongoing inflammation were only found in livers of SOD + Cho–fed animals (Figure 3). Thus, densitometric quantification of Sirius Red stains and quantification of the mRNA for *collagen type 1* (*Col1a1*) confirmed the presence of significantly elevated levels of collagen in SOD + Cho–fed animals (Figure 3A) compared with STD- or SOD-fed mice. Similarly, *transforming growth factor β1* (*Tgfb1*) mRNA was increased two-fold over the STD-fed animals. As a sign of enhanced apoptotic activity, the mRNA level of *Fas ligand* was increased more than two-fold only in livers of SOD + Cho–fed animals (Figure 3B), which is in line with the amplified TUNEL staining only in this group (Figure 2D). The histological signs of macrophage infiltration (Figure 1A, F4/80 staining) were confirmed by quantification of the mRNA levels of chemotactic chemokines and macrophage markers. Thus mRNA levels of *Ccl2* and *Cxcl2* were increased about six-fold (Figure 3C) and the mRNA for the monocyte/macrophage marker *F4/80* (*Adger1*) was increased five-fold (Figure 3D). Similarly, the mRNA for *Cd68*, which is expressed predominantly by phagocytic macrophages (M2), was increased five-fold, while the mRNA for *Cd11b* (*Itgam*), which is expressed predominantly by macrophages producing proinflammatory mediators (M1), was increased 2.5-fold (Figure 3D). In addition, the mRNAs for the proinflammatory cytokines *interleukin-1β* (*Il1b*) and *tumor necrosis factor α* (*Tnf*) as well as the IL-6-type cytokine *oncostatin M* (*Osm*) were elevated significantly four- to eight-fold in SOD + Cho–fed animals compared with STD- and SOD-fed mice (Figure 3E).

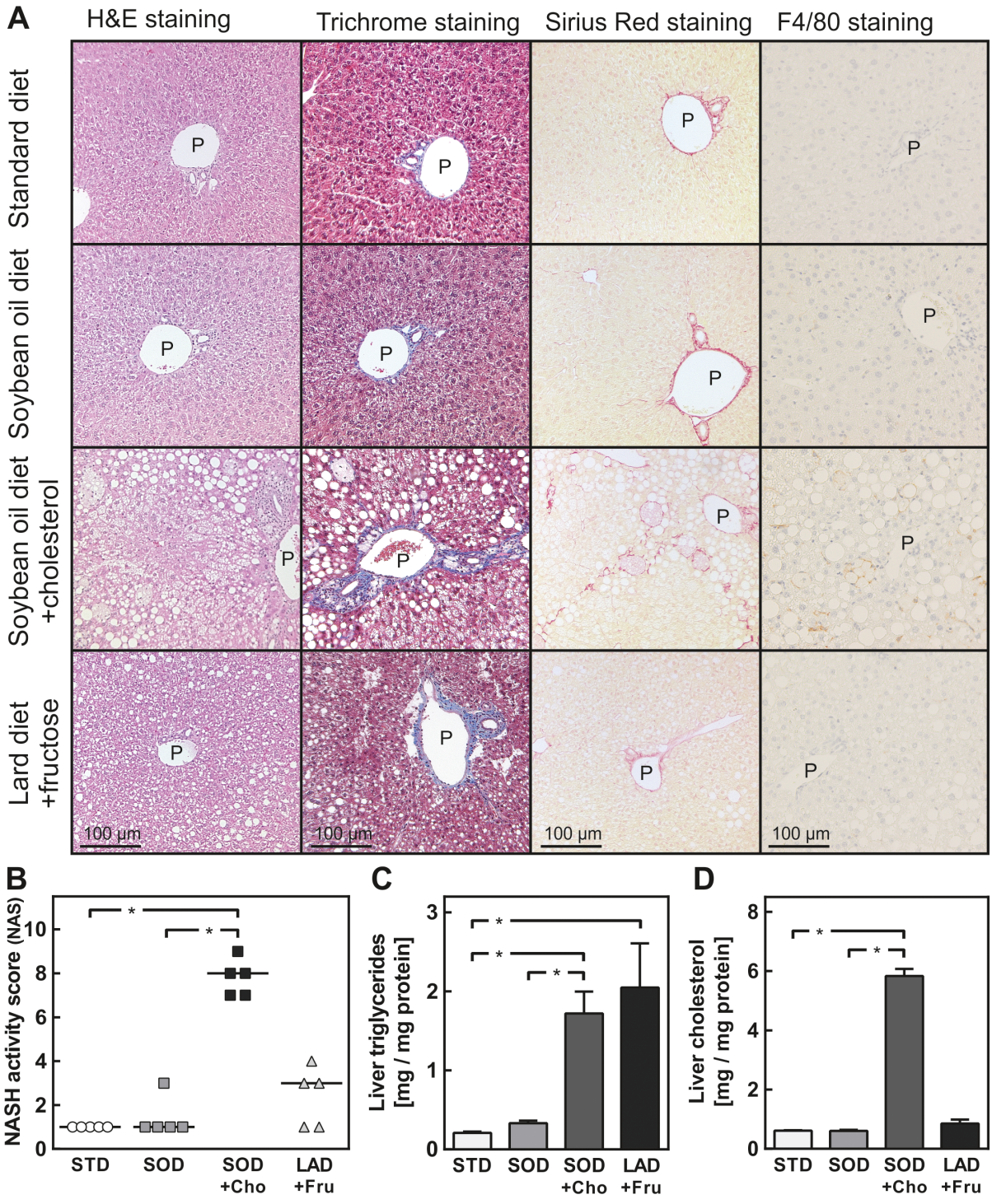

Figure 1. Dietary cholesterol in soybean oil diet enhanced NASH activity score, liver triglycerides and liver cholesterol. Mice were fed a standard diet (STD), soybean oil diet (SOD), soybean oil diet + 0.75% cholesterol (SOD + Cho) or lard diet + fructose in drinking water (LAD + Fru) for 20 wks. (A) Representative microphotographs of liver histology, magnification 20 ×. P: portal tract. (B) NASH activity score grading steatosis, ballooning (hypertrophy), inflammation and fibrosis. (C) Liver triglyceride and (D) liver cholesterol content per mg protein. Values represent (B) single score values and median per group or (C,D) mean ± standard error of the mean of 5 mice per group. Statistics: (B) Mann-Whitney U test, *p <0.05. (C, D) One-way analysis of variance with Dunnett's post hoc test or, where appropriate, Tukey's post hoc test for multiple comparisons, *p <0.05.

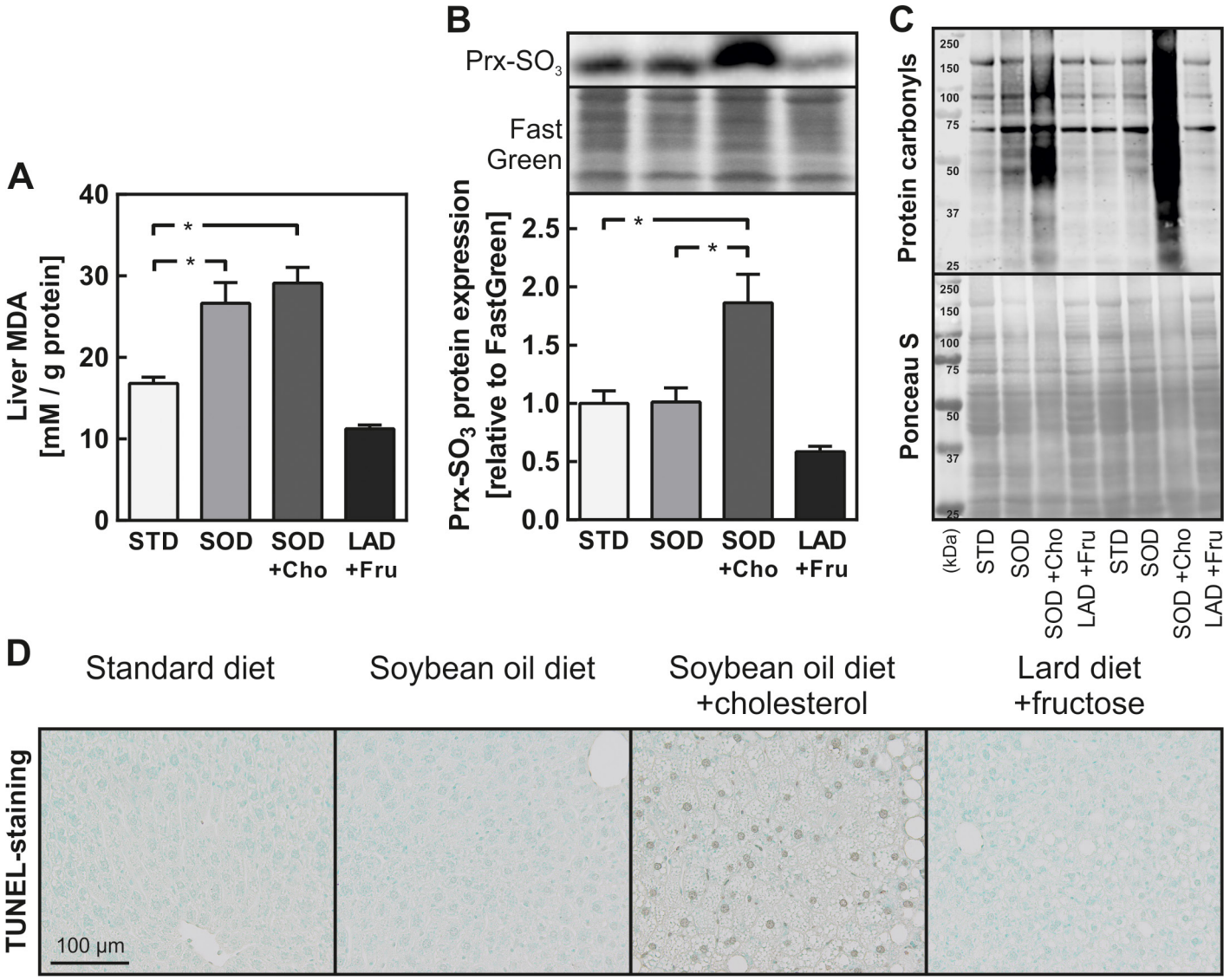

Figure 2. Dietary soybean oil diet increased hepatic lipid peroxidation, but only soybean oil diet + cholesterol provoked oxidative stress and apoptosis in mouse livers. Mice received diets as described in Figure 1. (A) Lipid peroxidation: malondialdehyde relative to protein content in liver homogenates. (B,C) Oxidative stress: hyperoxidized peroxiredoxins (Prx-SO_3, B) were determined in liver lysates by Western blot analysis with a specific antibody and normalized to Fast Green staining, which was verified on the same Western blot membrane as a loading control. Carbonylated proteins were verified by oxyblot with (C) ponceau S staining as a loading control. (D) Apoptosis: DNA damage in apoptotic cells was visualized by TUNEL staining. Values represent (A,B) means ± standard error of the mean of 5 mice per group or (C,D) representative photographs. Statistics: (A,B) One-way analysis of variance with Dunnett's post hoc test or, where appropriate, Tukey's post hoc test for multiple comparisons, *p <0.05.

Impact of Dietary Cholesterol in Soybean Oil Diet on Weight Gain and Body Composition

At the age of 8 wks, male mice were assigned to one of the diets. After adapting to the new diet for 1 wk, their weight gain under the respective diets was monitored for 19 wks. Weight gain was almost linear over the entire feeding period (see Supplementary Figure S1 for body weight curves). Due to glucose and insulin tolerance tests, which included fasting periods, weight gain in all groups was somewhat lower during the last 2 wks of the experiment. On average, animals fed STD gained 0.23 ± 0.03 g per week (Figure 4A). Weight gain was similar in animals fed SOD (0.20 ± 0.04 g/wk), whereas animals fed SOD + Cho gained significantly more weight (0.44 ± 0.05 g/wk, p <0.05). The fastest weight gain was

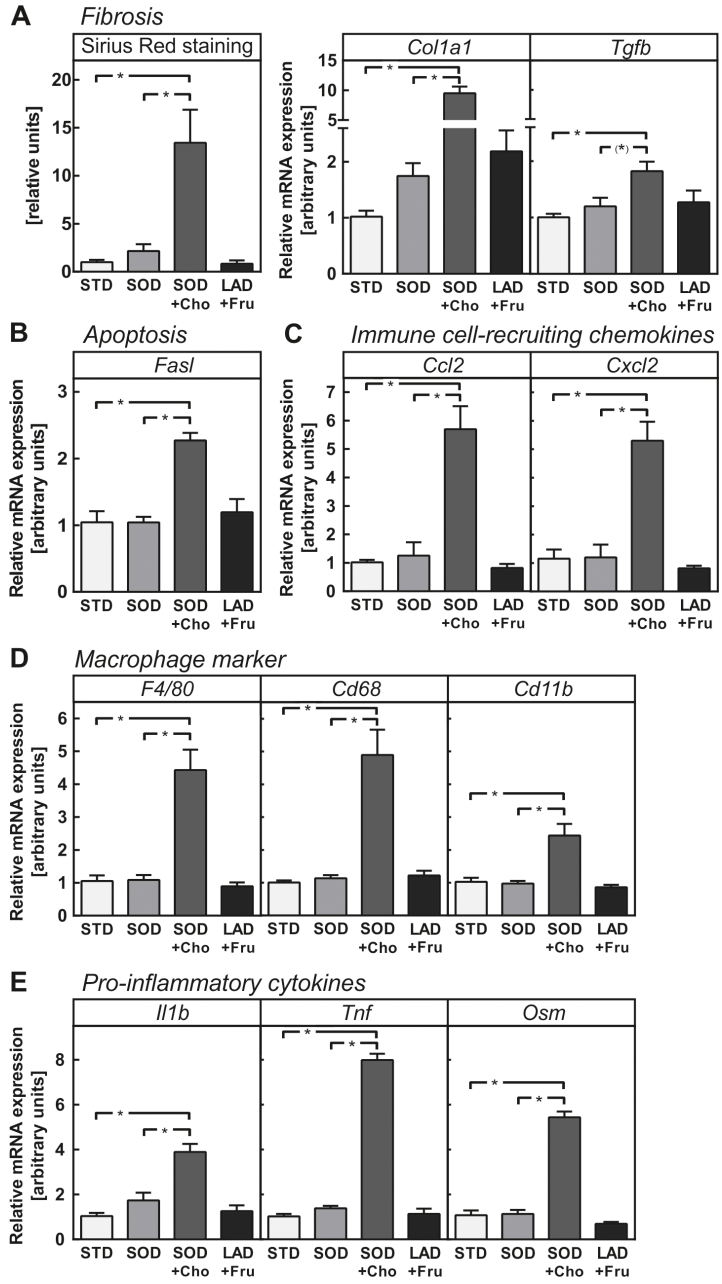

Figure 3. Dietary cholesterol in soybean oil diet increased hepatic fibrosis, apoptosis, macrophage infiltration and chemokine and cytokine production. Mice received diets as described in Figure 1. (A) Marker of fibrosis: quantification of Sirius Red–stained microphotographs, relative mRNA expression of *collagen type 1* (*Col1a1*) and *transforming growth factor β1* (*Tgfb1*). (B) Marker of apoptosis: relative mRNA expression of *Fas ligand* (*Fasl*). (C) Immune-cell recruiting chemokines: relative mRNA expression of *Ccl2* (*monocyte chemoattractant protein 1*, *Mcp-1*) and *Cxcl2* (*interleukin-8*, *Mip-2*). (D) Marker of macrophages: relative mRNA expression of macrophage surface proteins *F4/80* (*Adger1*), *Cd68* and *Cd11b* (*Itgam*). (E) Proinflammatory cytokines: relative mRNA expression of *interleukin-1β* (*Il1b*), *tumor necrosis factor α* (*Tnf*) and *oncostatin M* (*Osm*). Values represent means ± standard error of the mean of 5 mice per group. Statistics: One-way analysis of variance with Dunnett's post hoc test or, where appropriate, Tukey's post hoc test for multiple comparisons, *p <0.05, (*)p = 0.057.

observed in animals fed LAD + Fru (0.74 ± 0.08 g/wk, p <0.01).

The different diets resulted in different body compositions (Figure 4B). The relative fat mass of animals on STD was 3.2%. Animals on SOD had about 2.5-fold higher relative fat mass; however, the difference was not significant. By contrast, relative fat content was almost four-fold higher in animals receiving SOD + Cho than in animals receiving STD. Again, the highest relative body fat content was observed in animals receiving LAD + Fru, in which fat mass surpassed 27% of total body weight.

At variance with expectations, none of the high-fat diets resulted in an increase of plasma triglyceride levels or circulating free fatty acids (Supplementary Table S2, upper panel). This may be due to the marked hyperinsulinemia in these animals (see below), since very low-density lipoprotein synthesis in the liver is suppressed by high plasma insulin. Plasma cholesterol and low-density lipoprotein (LDL) cholesterol were significantly elevated in animals receiving LAD + Fru. There was also a trend toward an increase in SOD + Cho–fed animals, whereas neither cholesterol nor LDL cholesterol was altered in SOD-fed animals.

Induction of Insulin Resistance by Dietary Cholesterol in Soybean Oil Diet

Insulin sensitivity was determined in wk 18 by a glucose tolerance test with parallel determination of insulin plasma levels. As a measure of insulin resistance, the sum of the products of insulin concentration times glucose concentration was determined (Figure 4C). SOD-fed animals apparently were slightly more insulin resistant than STD-fed animals; however, this difference was not significant. By contrast, animals that received either SOD + Cho or LAD + Fru were significantly more insulin resistant than animals that received STD (Figure 4C). This was also reflected in the glucose tolerance curve alone (Supplementary Figure S2A). While the area under the curve for animals fed SOD did not differ

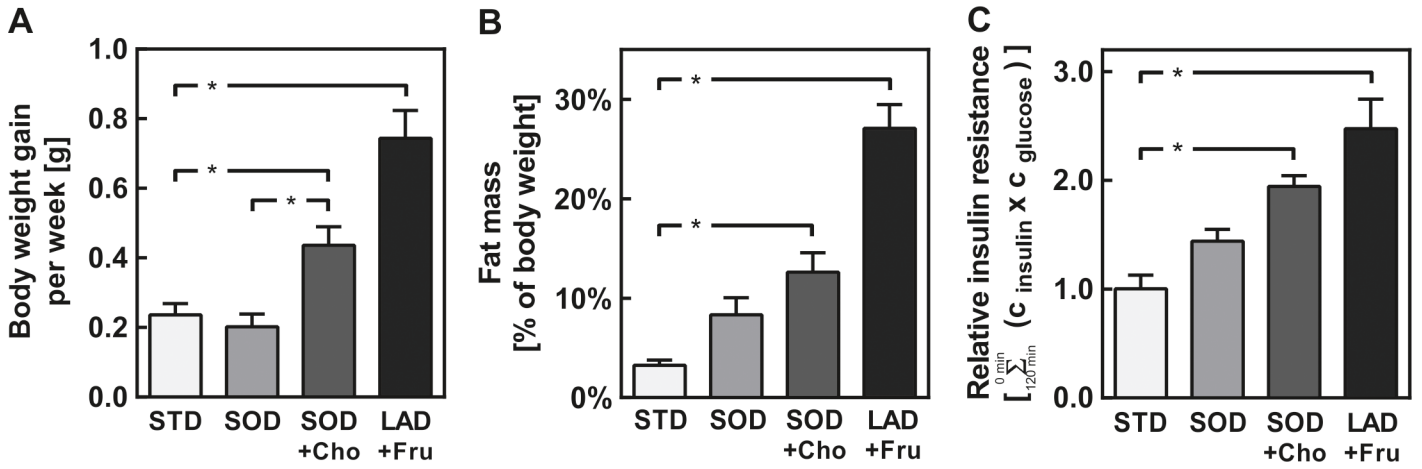

Figure 4. Increased weight gain, fat mass and insulin resistance in mice fed a soybean oil diet + cholesterol or a lard diet + fructose. Mice received diets as described in Figure 1. (A) Average body weight gain per week over 19 wks. (B) Fat mass in wk 20. (C) Relative insulin resistance was calculated by the sum of the products of insulin concentration × glucose concentration during oral glucose tolerance test. Values represent mean ± standard error of the mean of 5 mice per group. Statistics: One-way analysis of variance with Dunnett's post hoc test or, where appropriate, Tukey's post hoc test for multiple comparisons, *p <0.05.

significantly from those fed STD, animals that received SOD + Cho had a significantly elevated peak glucose value and a significantly higher area under the curve than animals that received STD (Supplementary Figure S2A). As expected from the body weight changes, animals that received LAD + Fru were the most glucose intolerant and were the only group in which the 120 min glucose value was significantly elevated compared to the STD control group (Supplementary Figure S2A). Animals that received SOD + Cho or LAD + Fru compensated for an apparent insulin resistance by increased endogenous insulin production (Supplementary Figure S2B). While the increased endogenous insulin production needed to maintain euglycemia or to cope with the glucose load during the oral glucose tolerance test indicated insulin resistance in SOD + Cho–fed animals, the drop in blood glucose levels during the insulin tolerance test in these animals was similar to that observed in SOD- and STD-fed animals (Supplementary Figure S2C). Only LAD + Fru–fed animals had significantly higher blood glucose levels during the entire course of the insulin tolerance test, resulting in a significantly greater area under the curve (Supplementary Figure S2C).

Impact of Dietary Cholesterol in Soybean Oil Diet on Hepatic Insulin Signaling

Previous data indicated that small lipid mediators such as arachidonic acid, (n-6)-derived prostanoids or palmitate-derived sphingolipids could inhibit hepatic insulin signaling and promote the development of hepatic insulin resistance and steatosis in isolated hepatocytes (20,27,28). Therefore, whether the apparent inflammation in the liver of SOD + Cho–fed animals had an impact on insulin signaling in the liver was tested. To this end, the protein levels of the key signal transduction molecules in the insulin receptor signal chain, the insulin receptor substrates 1 and 2 (IRS-1, IRS-2), were determined. While all three fat-rich diets reduced the IRS-1 level between 20% and 40% (Figure 5A), SOD had no impact on IRS-2. By contrast, IRS-2 expression on the protein level was almost completely abolished in SOD + Cho–fed animals (Figure 5B). IRS-2 was reduced also in LAD + Fru–fed animals, although not significantly. Whereas IRS-1 is predominantly involved in hepatic lipid metabolism, IRS-2 is the principal route for the insulin-dependent regulation of hepatic glucose metabolism. Thus, activation of glycogen synthesis is predominantly mediated via IRS-2. Presumably as a consequence of the reduced IRS-2 levels in livers of SOD + Cho–fed animals, glycogen content was significantly reduced in these animals, whereas it was similar to STD-fed animals in SOD- and LAD + Fru–fed animals (Figure 5C).

Possible Mechanism of Cholesterol-Induced Liver Inflammation

Since only SOD + Cho–fed animals showed signs of inflammation in the liver and these animals had the highest cholesterol content in liver tissue, whether hepatic cholesterol might directly trigger an inflammatory response was tested. To this end, Kupffer cells were isolated from control mice and exposed to cholesterol in culture. In accordance with the hypothesis, exposure of Kupffer cells to cholesterol crystals significantly induced expression of the chemotactic cytokines *Ccl2* and *Cxcl2* as well as the proinflammatory cytokines *Tnf* and *Osm* (Figures 6A and B). In

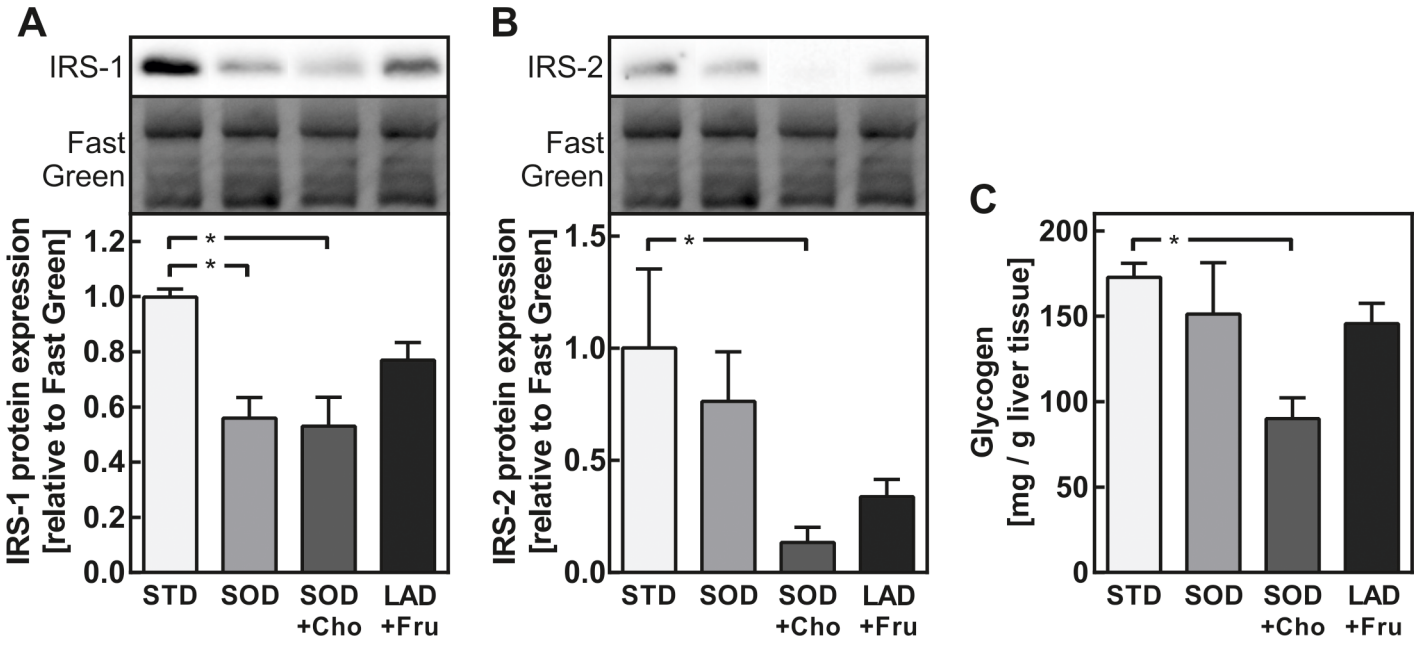

Figure 5. Dietary cholesterol in soybean oil diet impaired hepatic insulin signaling. Mice received diets as described in Figure 1. Protein levels of (A) insulin receptor substrate 1 (IRS-1) and (B) IRS-2 were determined in liver lysates by Western blot analysis with specific antibodies. Density units were normalized to Fast Green staining, which was verified on the same Western blot membrane as a loading control. (C) Hepatic glycogen content was enzymatically quantified in homogenates (see Materials and Methods section). Values represent means ± standard error of the mean of 5 mice per group. Statistics: One-way analysis of variance with Dunnett's post hoc test or, where appropriate, Tukey's post hoc test for multiple comparisons, *p <0.05.

contrast to whole livers of SOD + Cho–fed animals, *Il1b* was not induced (not shown). Thus, the strong inflammatory response in SOD + Cho–fed animals can possibly be explained in part by activation of Kupffer cells by the strongly elevated hepatic cholesterol levels in these animals.

Cholesterol not only induced an inflammatory response in Kupffer cells, but also increased the susceptibility of hepatocytes to a combination of pro-apoptotic signals. Therefore, actinomycin D augmented the caspase 3 activity in hepatocytes about three-fold. Neither TNFα nor cholesterol alone enhanced actinomycin D–stimulated caspase 3 activity significantly. However, if mouse hepatocytes were exposed to a combination of TNFα and cholesterol, the actinomycin D–dependent caspase 3 activity was significantly increased about two-fold (Figure 6C) and there was a significant interaction between cholesterol and TNFα (two-way analysis of variance, $p < 0.05$). Thus, cholesterol, in addition to triggering TNFα-production in Kupffer cells, also increased TNFα-dependent hepatocyte apoptosis.

DISCUSSION

Main Findings

The current study showed that a Western-type diet with high fat from soybean oil containing 0.75% cholesterol, in contrast to cholesterol-free high-fat diets with mainly saturated or high in polyunsaturated fatty acids, induced the development of NASH with inflammation and fibrosis (Figures 1, 2 and 3) in a mouse model that also developed overweight and displayed insulin resistance (Figure 4). Thus, this model, unlike other frequently used models (29,30), closely resembles the clinical features that accompany NASH in humans. In addition, the current model was developed on a wild-type C57BL/6 background, in contrast to several other models that showed the development of NASH on a monogenic mutant background that fostered the development of overweight (31,32), diabetes (33,34), hepatic lipid accumulation (35) or atherosclerosis (36) and hence might be strongly influenced by the special metabolic features of the mutant.

Dietary Cholesterol in Soybean Oil Diet as Main Trigger in NASH Development

The high-fat diets used in this study were different in their fatty acid composition as well as fructose and cholesterol content. Whereas the ratio of saturated to monounsaturated to polyunsaturated fatty acids was 32:39:29 in the lard-containing diet (LAD) as a typical high-fat diet, the ratio increased toward polyunsaturated fatty acids with 16:24:60 in SOD and SOD + Cho, defining them as Western-type diets. The fat source in the SOD and SOD + Cho diets was soybean oil, which is defined here as more

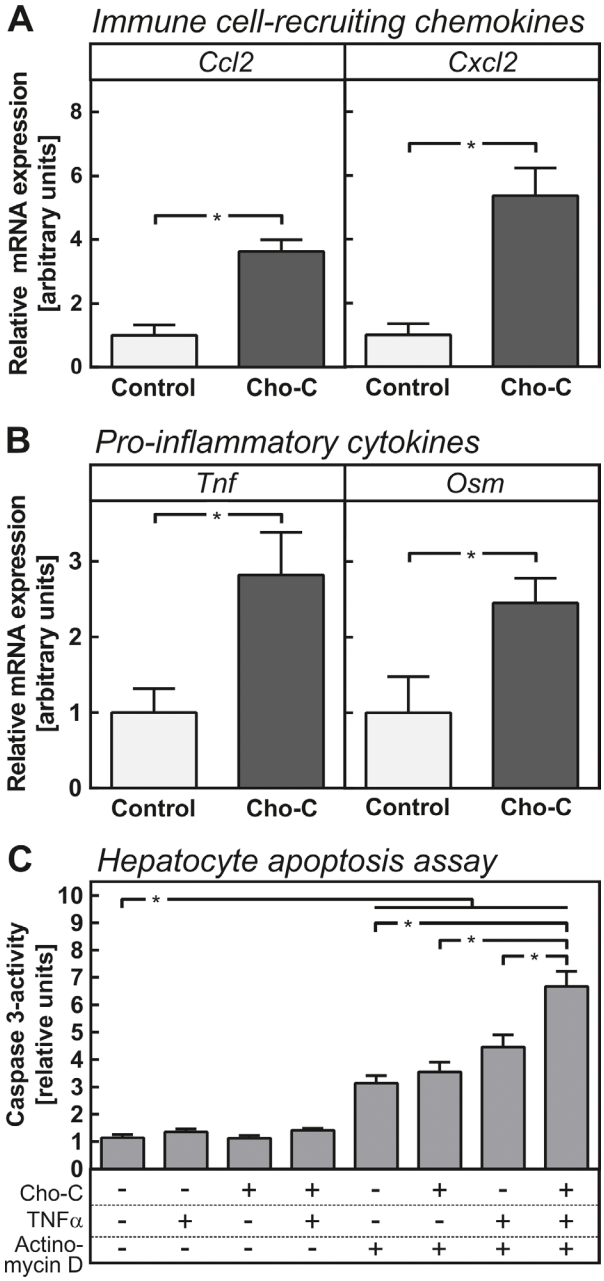

Figure 6. Cholesterol provoked a proinflammatory response in Kupffer cells and increased apoptosis in hepatocytes. (A,B) Primary mouse Kupffer cells were stimulated with 1 mg/mL cholesterol crystals (Cho-C) for 8 h. Relative mRNA expression levels of (A) the immune cell–recruiting chemokines *Ccl2* and *Cxcl2* and (B) the proinflammatory cytokines *tumor necrosis factor α* (*Tnf*) and *oncostatin M* (*Osm*) were quantified by RT-qPCR with *β-actin* (*Actb*) as reference gene. (C) Primary mouse hepatocytes were stimulated with 25 μg/mL cholesterol crystals (Cho-C), 1 ng/mL TNFα and 300 nM actinomycin D for 8 h. Apoptosis was determined by caspase 3 activity measured with a fluorescence-based assay and normalized to protein content. Values represent means ± standard error of the mean of a minimum of three independent experiments. Statistics: (A,B) Two-sided Student *t* test for unpaired samples, *p <0.05. (C) Two-sided Student *t* test for unpaired samples or, where appropriate, two-way analysis of variance with Tukey's post hoc test for multiple comparisons, *p <0.05.

obesogenic, diabetogenic and proinflammatory than fat sources such as lard or coconut oil with saturated fatty acids or fish oil with a different PUFA composition (13,14, 37–39). The high content of n-6-PUFA in soybean oil exaggerated insulin resistance and increased liver steatosis and inflammation in mice (38,14), while a high n-3/n-6-PUFA ratio in the diet reduced hepatic steatosis in humans and mice (39–41). n-6-fatty acids can be metabolized to arachidonic acid derivatives such as prostanoids (2-series) with proinflammatory properties, whereas n-3-fatty acids serve as substrates for less inflammatory prostanoids (3- and 5-series) or antiinflammatory metabolites (38,42). Serum levels of oxidized metabolites of the n-6 fatty arachidonic and linoleic acids were increased in mice fed a soybean oil–rich high-fat diet compared with mice fed a fish oil–rich high-fat diet (37). Furthermore, oxidized LDL caused Kupffer cell activation in a transgenic mouse model and thus might trigger hepatic inflammation (43). Alternatively, hepatocytes, which are damaged by oxidative stress, may activate Kupffer cells in their vicinity. Apparently the combination of intrahepatic accumulation of cholesterol with increased oxidative stress resulting from PUFA feeding was necessary to maximize oxidative stress and get the full proinflammatory and profibrotic response. In line with this hypothesis, markers of severe oxidative stress as opposed to mild signs of lipid peroxidation were only found in livers of SOD + Cho–fed mice, not in mice fed SOD, LAD + Fru (Figure 2A) or, as indicated by preliminary data, LAD + Cho (data not shown).

Fructose is discussed as acting as a dietary "second hit" in the progression from NAFLD to NASH (44). While fructose in combination with various high-fat diets augmented weight gain, insulin resistance and hepatic steatosis in feeding studies with rodents did not elicit hepatic inflammation or fibrosis (summarized in [44]). In this study, we tested a lard-containing high-fat diet supplemented with 5% fructose in drinking

water to aggravate the already described LAD-mediated hepatic steatosis, but in line with other studies, the LAD + Fru–fed mice display only an NAFLD-phenotype with steatosis and without inflammation and fibrosis (Figure 1).

In the current study, both SOD and LAD + Fru induced only simple hepatosteatosis without any signs of inflammation, whereas SOD + Cho caused steatosis and inflammation accompanied by increased oxidative stress. Thus, dietary cholesterol might be an important trigger of the inflammatory response in the liver, particularly in an environment prone to lipid peroxidation. In accordance with such a hypothesis, other diets that have a comparatively high cholesterol content, such as a cafeteria diet (12,45) or a cholesterol-enriched high-fat diet (46), have been reported to induce NASH-like symptoms in mice. However, there was no insulin resistance or glucose intolerance in the latter (46). By contrast, ezitimibe, an inhibitor of enteral cholesterol uptake, improved liver pathology on a high-fat, high-cholesterol diet (47). The notion that dietary cholesterol might directly affect the progression of NASH is further supported by the observation that although plasma cholesterol and LDL cholesterol were higher in LAD + Fru–fed animals (Supplementary Table S2) and hepatic triglyceride levels were identical in LAD + Fru– and SOD + Cho–fed animals, hepatic cholesterol levels were particularly high in SOD + Cho–fed animals (Figures 1C and D), indicating that the oral route of cholesterol delivery resulted in an accumulation of cholesterol in the liver.

Direct and Indirect Stimulation of Macrophage Inflammatory Response by Cholesterol

The high hepatic content of cholesterol might directly stimulate an inflammatory response in the liver. In support of this, previous studies by us (48) and others (34,36,49) have shown that atherogenic diets rich in cholesterol, which are usually used in cardiovascular disease models, induced expression of proinflammatory cytokines in the liver. Similarly, both chemotactic and proinflammatory cytokines were induced in livers of SOD + Cho–fed animals, and histological analysis visualized Kupffer cells aggregated around lipid-overloaded hepatocytes, forming similar "crown-like-structure" constructs (Figure 3). In extension of these observations, the current study shows that expression of chemotactic and proinflammatory cytokines was induced in Kupffer cells by cholesterol and cholesterol crystals (Figures 6A and B). Cholesterol crystals have been shown to be in fat droplets in hepatocytes in patients with NASH as well as in mice fed a high-fat high-cholesterol diet (50). This might be responsible for stimulating an inflammatory response in Kupffer cells, which take up the debris of necrotic or apoptotic hepatocytes, and has been discussed as a key mechanism in the progression from NAFLD to NASH (50,51). Similarly, it has recently been shown that accumulation of toxic lipids in Kupffer cells contributes to the development of inflammation in early stages of NASH (52). In addition, excess cholesterol and cholesterol crystals can directly activate the NLRP3-inflammasome in macrophages, thereby enhancing the proinflammatory response and promoting development to hepatic steatohepatitis (24,53).

Cholesterol-Dependent Increase in Hepatocyte Apoptosis Sensitivity

Cholesterol not only enhanced the inflammatory response, it apparently rendered hepatocytes more sensitive to pro-apoptotic stimuli (Figure 6C). This is in accordance with previous reports in the literature: a cholesterol-containing diabetogenic high-fat diet increased the number of apoptotic hepatocytes in livers of LDL receptor–deficient mice more than a cholesterol-free diabetogenic diet of otherwise similar composition (36). Similarly, a correlation was found between hepatic cholesterol content and apoptosis in a porcine animal model of NAFLD (54).

Possible Contribution of Insulin Resistance to Hepatic Cholesterol Load

The SOD + Cho–fed animals apparently were insulin resistant and had elevated plasma insulin levels after exposure to glucose in the glucose tolerance test (Supplementary Figure S2). Insulin resistance and the ensuing hyperinsulinemia may further contribute the accumulation of cholesterol in the livers of animals fed the SOD + Cho diet. Insulin has been shown to increase the uptake of cholesterol into hepatocytes by inducing the LDL receptor and impeding the elimination of cholesterol by downregulating the enzymes involved in the conversion of cholesterol into bile acids and the cholesterol export pumps (34). Hyperinsulinemia, in addition, has recently been shown to induce expression of proinflammatory cytokines in macrophages (19), thereby further aggravating intrahepatic inflammation in a vicious cycle.

CONCLUSION

In summary, adding cholesterol to a high-fat and high–n-6-PUFA diet fed to normal C57BL/6 mice induces pathology that closely resembles NASH in humans suffering from the metabolic syndrome and might thus be a suitable model to study the mechanisms underlying disease development or to test therapeutic interventions. Further studies are necessary to determine the effects of dietary cholesterol alone and the role of fatty acid composition in high-fat diets.

ACKNOWLEDGMENTS

The excellent technical work of Manuela Kuna, Ines Grüner, Elisabeth Meyer and Susann Richter is gratefully acknowledged.

DISCLOSURE

The authors declare they have no competing interests as defined by *Molecular Medicine* or other interests that might be perceived to influence the results and discussion reported in this paper. This work was funded in part by the German Research Foundation (grant HE-7032/1-1).

REFERENCES

1. Püschel GP, Jungermann K. (1994) Integration of function in the hepatic acinus: intercellular communication in neural and humoral control of liver metabolism. *Prog. Liver Dis.* 12:19–46
2. Postic C, Dentin R, Girard J. (2004) Role of the liver in the control of carbohydrate and lipid homeostasis. *Diabetes Metab*. 30:398–408.
3. Dowman JK, Tomlinson J, Newsome P. (2010) Pathogenesis of non-alcoholic fatty liver disease. *QJM.* 103:71–83.
4. World Gastroenterology Organisation. (2012) Nonalcoholic Fatty Liver Disease and Nonalcoholic Steatohepatitis. World Gastroenterology Organisation Global Guidelines 2012.
5. Brunt EM. (2010) Pathology of nonalcoholic fatty liver disease. *Nat. Rev. Gastroenterol. Hepatol.* 7:195–203.
6. Tilg H, Moschen AR. (2010) Evolution of inflammation in nonalcoholic fatty liver disease: the multiple parallel hits hypothesis. *Hepatology.* 52:1836–46.
7. Sanches SCL, Ramalho LNZ, Augusto MJ, da Silva DM, Ramalho FS. (2015) Nonalcoholic Steatohepatitis: A Search for Factual Animal Models. *BioMed. Res. Int.* 2015:574832.
8. Ikejima K, et al. (2005) The role of leptin in progression of non-alcoholic fatty liver disease. *Hepatol. Res*. 33:151–54.
9. Hebbard L, George J. (2011) Animal models of nonalcoholic fatty liver disease. *Nature Rev. Gastroenterol. Hepatol.* 8:35–44.
10. Reid DT, Eksteen B. (2015) Murine models provide insight to the development of non-alcoholic fatty liver disease. *Nutr. Res. Rev*. 28:133–42.
11. Spruss A, et al. (2012) Female mice are more susceptible to nonalcoholic fatty liver disease: sex-specific regulation of the hepatic AMP-activated protein kinase-plasminogen activator inhibitor 1 cascade, but not the hepatic endotoxin response. *Mol. Med.* 18:1346–55.
12. Charlton M, et al. (2011) Fast food diet mouse: novel small animal model of NASH with ballooning, progressive fibrosis, and high physiological fidelity to the human condition. *Am. J. Physiol. Gastrointest. Liver Physiol.* 301:G825–34.
13. Deol P, et al. (2015) Soybean Oil Is More Obesogenic and Diabetogenic than Coconut Oil and Fructose in Mouse: Potential Role for the Liver. *PLoS One.* 10:e0132672.
14. Midtbo LK, *et al.* (2013) Intake of farmed Atlantic salmon fed soybean oil increases insulin resistance and hepatic lipid accumulation in mice. *PLoS One.* 8:e53094.
15. Weber D, et al. (2014) Oxidative stress markers and micronutrients in maternal and cord blood in relation to neonatal outcome. *Eur. J. Clin. Nutr.* 68:215–22.
16. Kleiner DE, *et al.* (2005) Design and validation of a histological scoring system for nonalcoholic fatty liver disease. *Hepatology*. 41:1313–21.
17. Liang W, et al. (2014) Establishment of a general NAFLD scoring system for rodent models and comparison to human liver pathology. *PLoS One*. 9:e115922.
18. Schneider CA, Rasband WS, Eliceiri KW. (2012) NIH Image to ImageJ: 25 years of image analysis. *Nature Meth*. 9: 671–75.
19. Manowsky J, Camargo RG, Kipp AP, Henkel J, Püschel GP. (2016) Insulin-induced cytokine production in macrophages causes insulin resistance in hepatocytes. *Am. J. Physiol. Endocrinol. Metab.* 310:E938–46.
20. Henkel J, Neuschäfer-Rube F, Pathe-Neuschäfer-Rube A, Püschel GP. (2009) Aggravation by prostaglandin E2 of interleukin-6-dependent insulin resistance in hepatocytes. *Hepatology.* 50:781–90.
21. Castro JP, Ott C, Jung T, Grune T, Almeida H. (2012) Carbonylation of the cytoskeletal protein actin leads to aggregate formation. *Free Rad. Biol. Med.* 53:916–25.
22. Fennekohl A, et al. (2002) Contribution of the two Gs-coupled PGE2-receptors EP2-receptor and EP4-receptor to the inhibition by PGE2 of the LPS-induced TNFalpha-formation in Kupffer cells from EP2-or EP4-receptor-deficient mice. Pivotal role for the EP4-receptor in wild type Kupffer cells. *J. Hepatol.* 36:328–34.
23. Froh M, Konno A, Thurman RG. (2003) Isolation of liver Kupffer cells. *Curr. Protoc. Toxicol*. 14:14.4.1–12.
24. Rajamaki K, et al. (2010) Cholesterol crystals activate the NLRP3 inflammasome in human macrophages: a novel link between cholesterol metabolism and inflammation. *PLoS One*. 5(7):e11765.
25. Bradford MM. (1976) A rapid and sensitive method for the quantitation of microgram quantities of protein utilizing the principle of protein-dye binding. *Anal. Biochem*. 72:248–54.
26. Cadenas E, Packer L, eds. (2010) *Thiol Redox Transitions in Cell Signaling, Part B: Cellular Localization and Signaling*. Boston: Elsevier. 340 pp.
27. Henkel J, et al. (2012) Stimulation of fat accumulation in hepatocytes by PGE(2)-dependent repression of hepatic lipolysis, beta-oxidation and VLDL-synthesis. *Lab. Invest.* 92:1597–1606.
28. Fayyaz S, et al. (2014) Involvement of sphingosine 1-phosphate in palmitate-induced insulin resistance of hepatocytes via the S1P2 receptor subtype. *Diabetologia.* 57:373–82.
29. Rinella ME, et al. (2008) Mechanisms of hepatic steatosis in mice fed a lipogenic methionine choline-deficient diet. *J. Lipid Res*. 49:1068–76.
30. Ramadori P, Weiskirchen R, Trebicka J, Streetz K. (2015) Mouse models of metabolic liver injury. *Lab. Anim*. 49(1 Suppl):47–58.
31. Yang SQ, Lin HZ, Lane MD, Clemens M, Diehl AM. (1997) Obesity increases sensitivity to endotoxin liver injury: implications for the pathogenesis of steatohepatitis. *Proc. Natl. Acad. Sci. USA*. 94:2557–62.
32. Wortham M, He L, Gyamfi M, Copple BL, Wan YY. (2008) The transition from fatty liver to NASH associates with SAMe depletion in db/db mice fed a methionine choline-deficient diet. *Dig. Dis. Sci.* 53:2761–74.
33. Okumura K, et al. (2006) Exacerbation of dietary steatohepatitis and fibrosis in obese, diabetic KK-A(y) mice. *Hepatol. Res*. 36:217–28.
34. van Rooyen DM, et al. (2011) Hepatic free cholesterol accumulates in obese, diabetic mice and causes nonalcoholic steatohepatitis. *Gastroenterology.* 141:1393–403, e1–5.
35. Nakayama H, et al. (2007) Transgenic mice expressing nuclear sterol regulatory element-binding protein 1c in adipose tissue exhibit liver histology similar to nonalcoholic steatohepatitis. *Metab. Clin. Exp*. 56:470–75.
36. Subramanian S, *et al.* (2011) Dietary cholesterol exacerbates hepatic steatosis and inflammation in obese LDL receptor-deficient mice. *J. Lipid Res*. 52(9): 1626–35.
37. Lazic M, et al. (2014) Reduced dietary omega-6 to omega-3 fatty acid ratio and 12/15-lipoxygenase deficiency are protective against chronic high fat diet-induced steatohepatitis. *PLoS One.* 9:e107658.
38. Midtbo LK, *et al.* (2015) Intake of farmed Atlantic salmon fed soybean oil increases hepatic levels of arachidonic acid-derived oxylipins and ceramides in mice. *J. Nutr. Biochem*. 26:585–95.
39. Rossmeisl M, *et al.* (2014) Omega-3 phospholipids from fish suppress hepatic steatosis by integrated inhibition of biosynthetic pathways in dietary obese mice. *Biochim. Biophys. Acta.* 1841:267–78.
40. Parker HM, (2012) Omega-3 supplementation and non-alcoholic fatty liver disease: a systematic review and meta-analysis. *J. Hepatol*. 56:944–51.
41. Lee HJ, et al. (2016) Dietary Black Raspberry Seed Oil Ameliorates Inflammatory Activities in db/db Mice. *Lipids*. 51:715–27.
42. Calder PC. (2009) Polyunsaturated fatty acids and inflammatory processes: New twists in an old tale. *Biochimie*. 91:791–95.
43. Bieghs V, et al. (2012) Specific immunization strategies against oxidized low-density lipoprotein: a novel way to reduce nonalcoholic steatohepatitis in mice. *Hepatology*. 56:894–903.
44. Longato L. (2013) Non-alcoholic fatty liver disease (NAFLD): a tale of fat and sugar? *Fibrogenesis Tissue Repair*. 6:14.
45. Sampey BP, et al. (2011) Cafeteria diet is a robust model of human metabolic syndrome with liver and adipose inflammation: comparison to high-fat diet. *Obesity*. 19:1109–17.
46. Savard C, et al. (2013) Synergistic interaction of dietary cholesterol and dietary fat in inducing experimental steatohepatitis. *Hepatology*. 57:81–92.
47. Zheng S, et al. (2008) Ezetimibe improves high fat and cholesterol diet-induced non-alcoholic fatty liver disease in mice. *Eur. J. Pharmacol*. 584:118–24.
48. Henkel J, et al. (2011) Oncostatin M produced in Kupffer cells in response to PGE2: possible contributor to hepatic insulin resistance and steatosis. *Lab. Invest*. 91:1107–17.
49. Matsuzawa N, *et al*. (2007) Lipid-induced oxidative stress causes steatohepatitis in mice fed an atherogenic diet. *Hepatology*. 46:1392–1403.

50. Ioannou GN, Haigh WG, Thorning D, Savard C. (2013) Hepatic cholesterol crystals and crown-like structures distinguish NASH from simple steatosis. *J. Lipid Res*. 54:1326–34.
51. Ioannou GN (2016) The Role of Cholesterol in the Pathogenesis of NASH. *Trends Endocrin. Met*. 27:84–95.
52. Leroux A, *et al*. (2012) Toxic lipids stored by Kupffer cells correlates with their pro-inflammatory phenotype at an early stage of steatohepatitis. *J. Hepatol*. 57:141–49.
53. Duewell P, *et al.* (2010) NLRP3 inflammasomes are required for atherogenesis and activated by cholesterol crystals. *Nature*. 464:1357–61.
54. Liang T, *et al*. (2015) Liver injury and fibrosis induced by dietary challenge in the Ossabaw miniature swine. *PLoS ONE*. 10:e0124173.

Cite this article as: Henkel J, *et al.* (2017) Induction of steatohepatitis (NASH) with insulin resistance in wild-type B6 mice by a western-type diet containing soybean oil and cholesterol. *Mol. Med*. 23:70–82.